Association between regional monsoon onset in South Asia and Tibetan Plateau thermal forcing

Die Hu
State Key Laboratory of Numerical Modeling for Atmospheric Sciences and Geophysical Fluid Dynamics

Anmin Duan (amduan@lasg.iap.ac.cn)
Institute of Atmospheric Physics (IAP) https://orcid.org/0000-0002-3022-2582

Ping Zhang
State Key Laboratory of Numerical Modeling for Atmospheric Sciences and Geophysical Fluid Dynamics

Research Article

Keywords: Tibetan Plateau, thermal forcing, South Asian summer monsoon, onset

Posted Date: May 13th, 2021

DOI: https://doi.org/10.21203/rs.3.rs-398584/v1

Abstract

By using multiple data sources and two sensitivity experiments using the atmospheric general circulation model of CAM4.0, we investigated the effect of thermal forcing over the Tibetan Plateau (TP) on the onset of the South Asian summer monsoon, including over the Arabian Sea (AS) and India. Results indicate that the seesaw pattern of diabatic heating over the TP, with a southeastern–northwestern inverse distribution in May, shows a robust relationship with the date of monsoon onset over the AS and India, which is independent of the influences from ocean signals. A positive diabatic heating seesaw pattern can enhance the ascending (descending) motion over the southeastern (northwestern) TP, corresponding to above (below) normal in- situ precipitation. Temperature budget diagnosis reveals that the adiabatic heating by the anomalous vertical motion and relevant horizontal advection of temperature convergence in the mid-upper troposphere are contributors to the warming over the TP. Consequently, the transition of the meridional temperature gradient over South Asian regions occurs earlier. Furthermore, the diabatic heating over the TP induces an enhanced and westward-extended South Asian high (SAH), which together with the easterly along the southern flank of the SAH superimpose on the low-level westerly flow over the AS and India, resulting in intensive upper-level divergence-pumping and upward motion. This anomalous circulation configuration in lower and upper levels further facilitates an earlier onset of summer monsoon in these two regions. These findings are corroborated in the sensitivity runs based on CAM4.0.

Full Text

This preprint is available for download as a PDF.

Figures

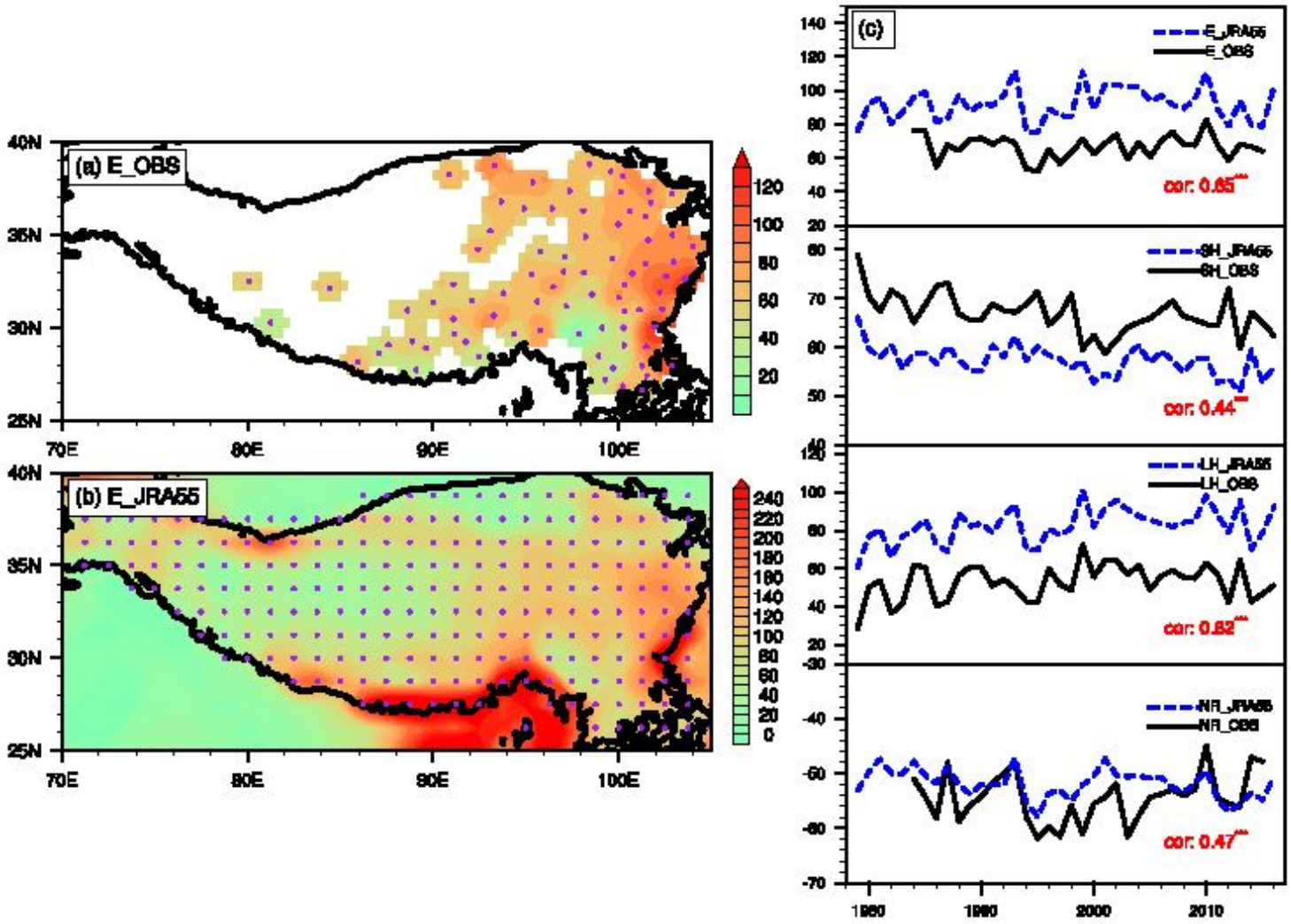

Figure 1

Climatological spatial patterns (a and b) and time series (c) of the atmospheric heat source/sink (E), sensible heat (SH), latent heat (LH) and net radiation (NR) over the TP in May based on (a) observed datasets and (b) JRA-55 datasets. The purple dots in (a) and (b) represent the distribution of the 80 routine weather stations and TP areas with an altitude > 2000 m, respectively. The solid black curve denotes the 80-station average E, SH, LH and NR based on the observed datasets, and the blue dotted curve denotes the dot areas' averaged E, SH, LH and NR based on JRA-55 in (b), and the correlation

coefficients between them are marked in the third panel. The black contours in (a) and (b) indicate the 2000 m topographic height

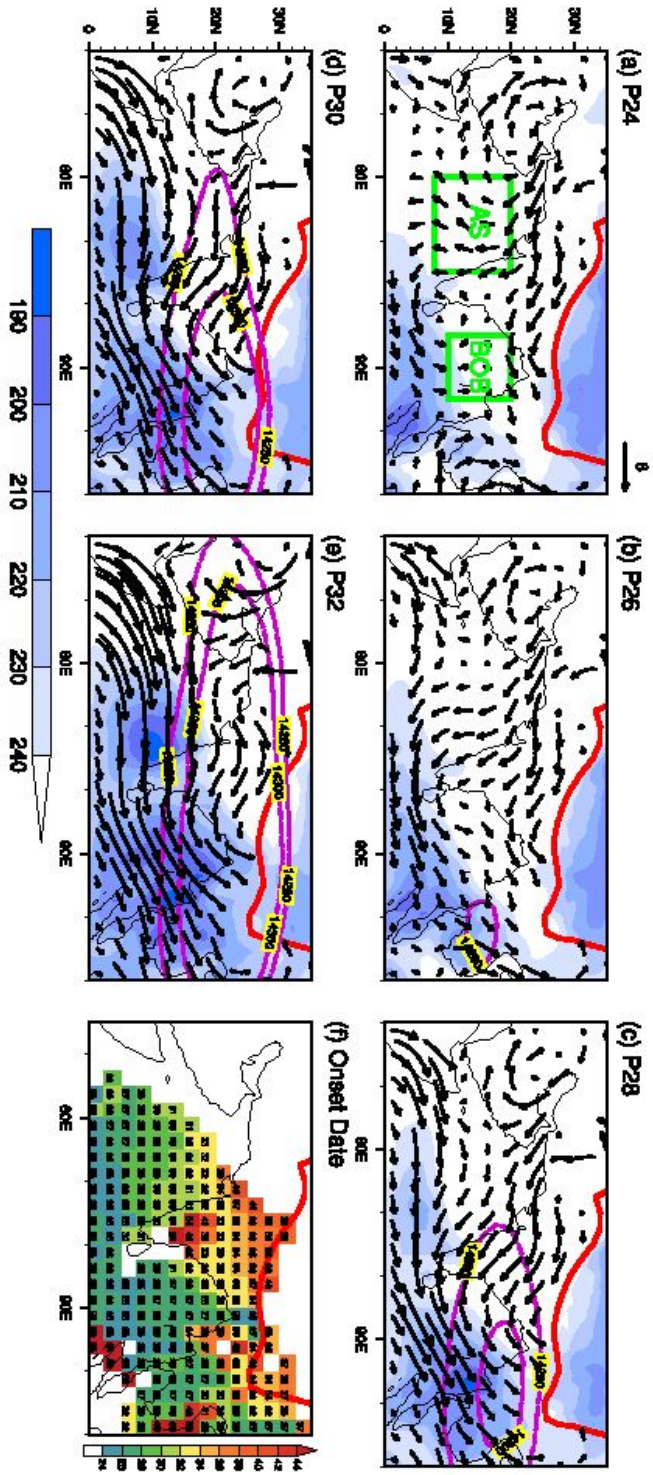

Figure 2

Climate-mean pentad OLR (shading, units: W m−2) and 850-hPa wind (vectors, units: m s−1) in the antecedent evolution of the SASM onset from pentad 24 to 32 (a–e). Magenta contours in (a–e) represent the 14280 and 14300 geopotential heights. The green boxes indicate the AS and BOB regions.

(f) Dates of onset determined by the relative pentad-mean rainfall rate. The red contour indicates the 2000 m topographic height

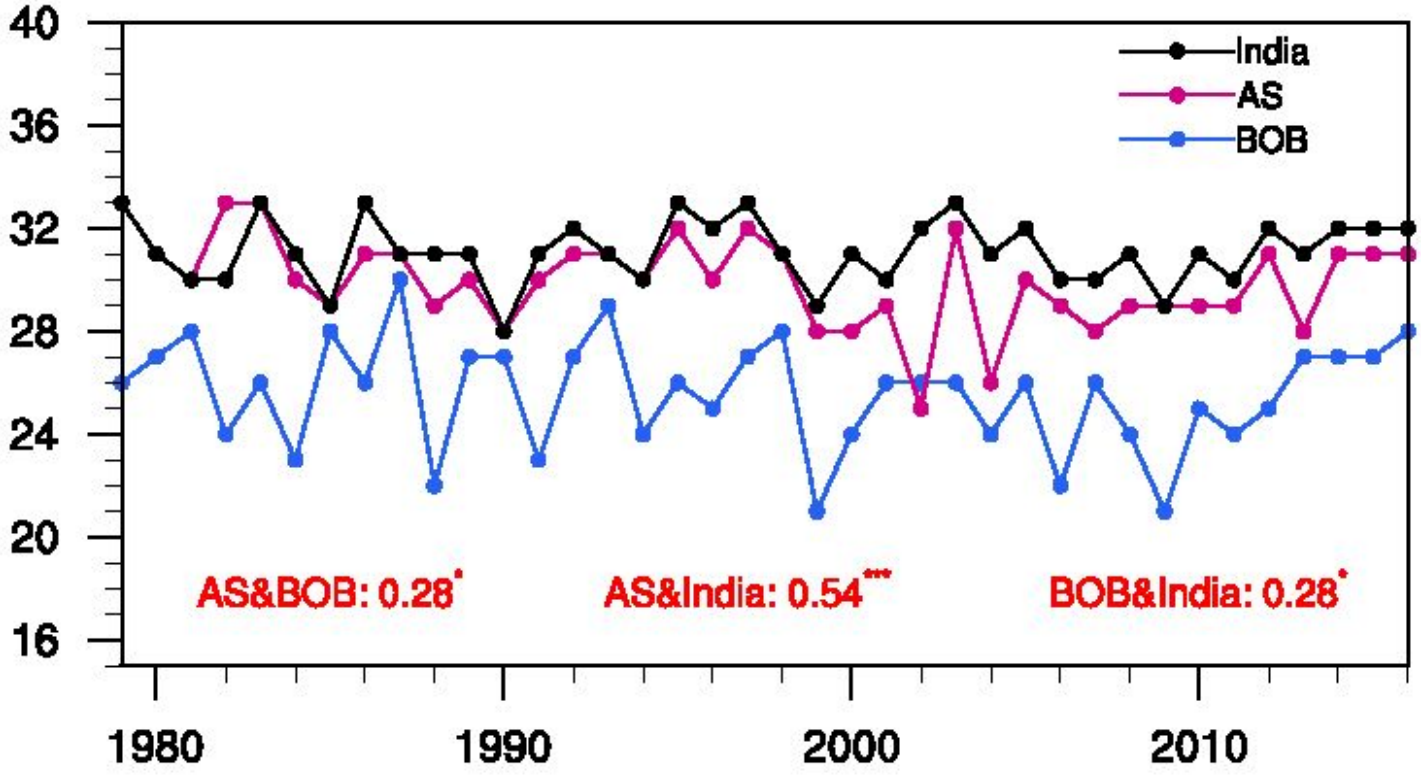

Figure 3

Time series of summer monsoon onset dates. The magenta, blue and black curves represent the summer monsoon onset over the AS, BOB and India, respectively. The onset dates of the summer monsoon over the AS and BOB are based on the method of Wang and LinHo (2002), while the Indian summer monsoon onset is from the Indian Meteorological Department. The correlation coefficients between them during the

period 1979–2016 are marked at the bottom of each panel. Statistical significance is shown by asterisks: * p < 0.1, ** p < 0.05 and *** p < 0.01 (the same hereafter).

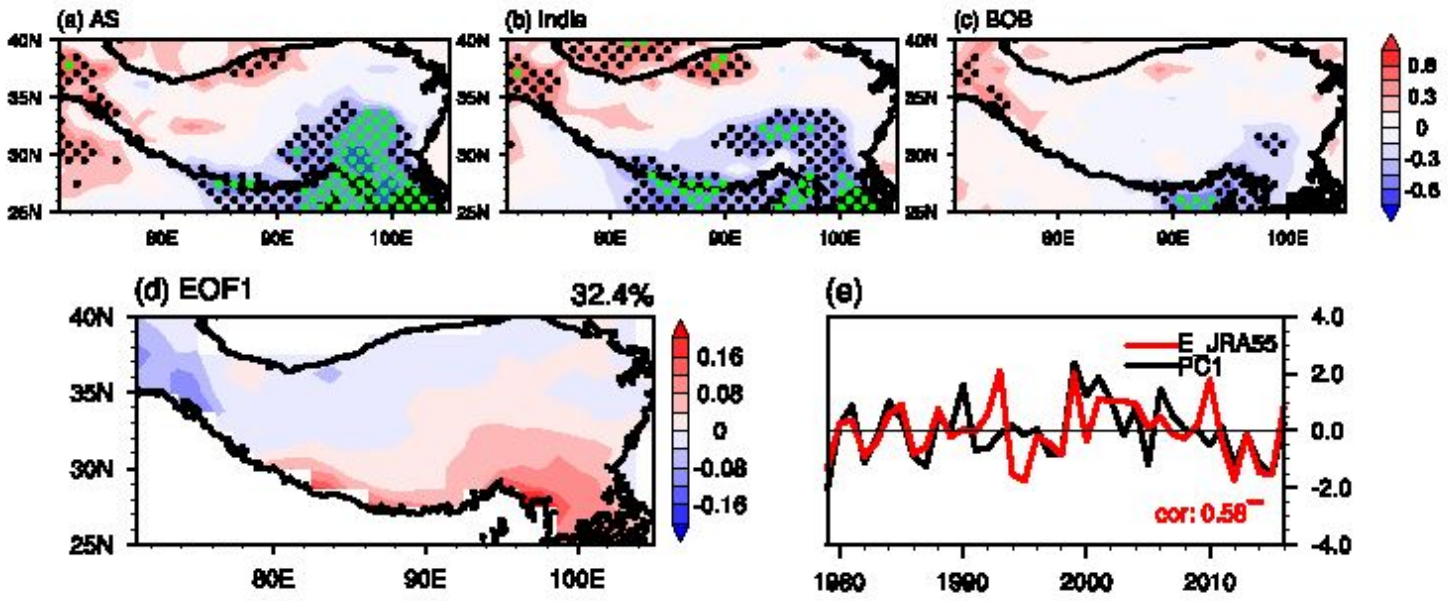

Figure 4

Correlation pattern between the atmospheric heat source/sink (E) over the TP in May and summer monsoon onset over (a) the AS, (b) India, and (c) the BOB. (d) First EOF mode of the atmospheric heat source/sink over the TP (> 2000 m) in May during 1979–2016 based on JRA-55 datasets, and (e) the time series of PC1 and E_JRA55, with the correlation coefficient between them during the period 1979–

2016 marked in (e). The value in the upper right is the explained variance of the mode. Black and green dotted areas in (a–c) are where the statistical significance passed the 90% and 95% confidence levels, respectively. The black contours in (a) and (b) indicate the 2000 m topographic height

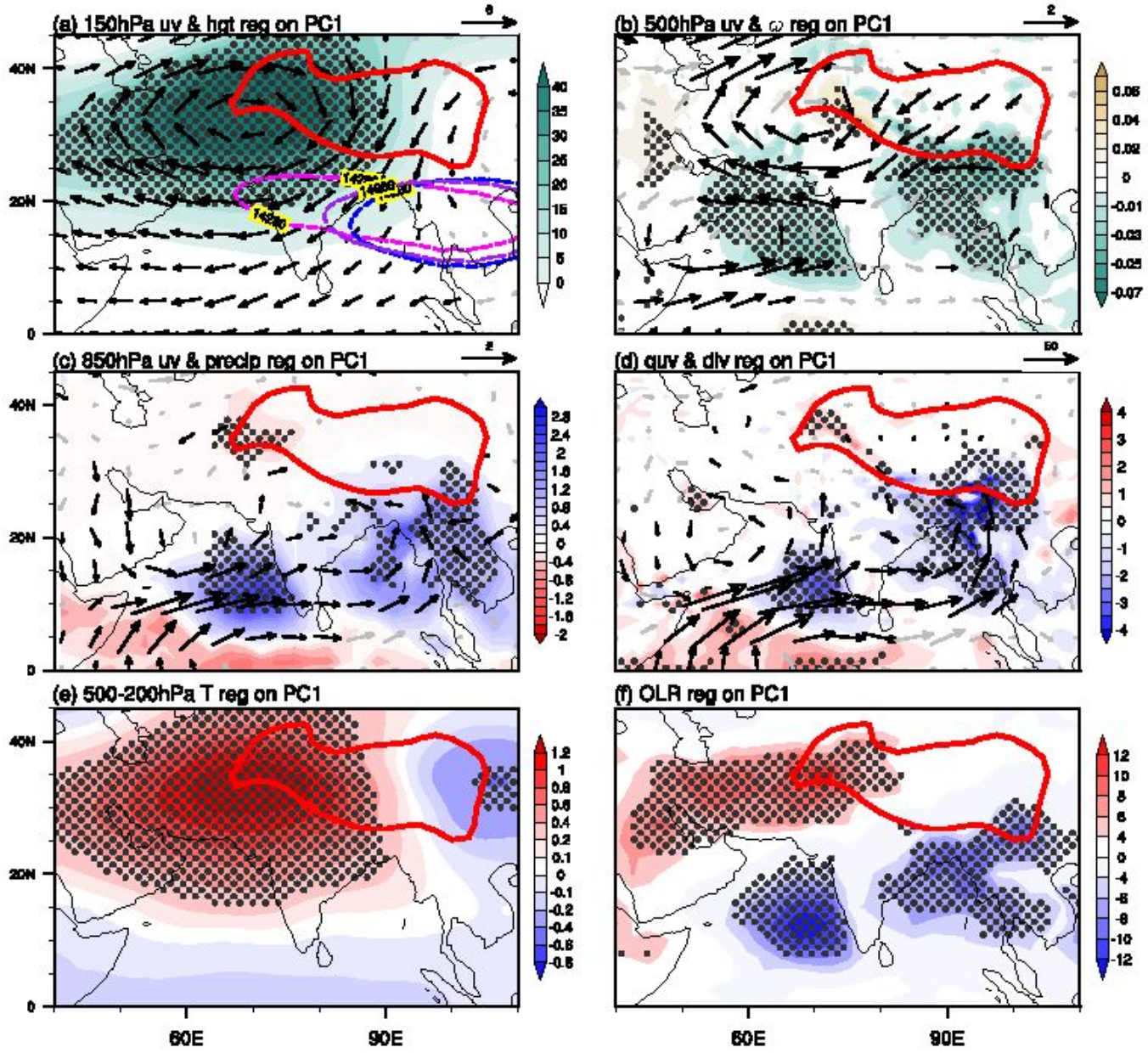

Figure 5

Regression of May quantities against the PC1 corresponding to EOF1 of the atmospheric heat source over the TP in May during 1979–2016: (a) 150-hPa geopotential height (shading, unit: gpm) and 150-hPa wind (vectors, units: m s−1); (b) 500-hPa vertical velocity (shading, units: Pa s−1) and 500-hPa wind

(vectors, units: m s−1); (c) precipitation (shading, units: mm day−1) and 850-hPa wind (vectors, units: m s−1); (d) surface to 100-hPa vertically integrated moisture divergence (shading, units: 10−5 kg m−2 s−1) and moisture transport anomalies (vectors, units: kg m−1 s−1); (e) temperature vertically averaged over 500–200 hPa (shading, unit: K); and (f) OLR (shading, units: W m−2). The purple, magenta and blue contours in (a) indicate the composite 14280 geopotential heights in the climatology, in positive PC1 years and negative PC1 years. Black dotted areas and black vectors indicate statistical significance at or above the 99% confidence level. The black contours in (a) and (b) indicate the 2000 m topographic height

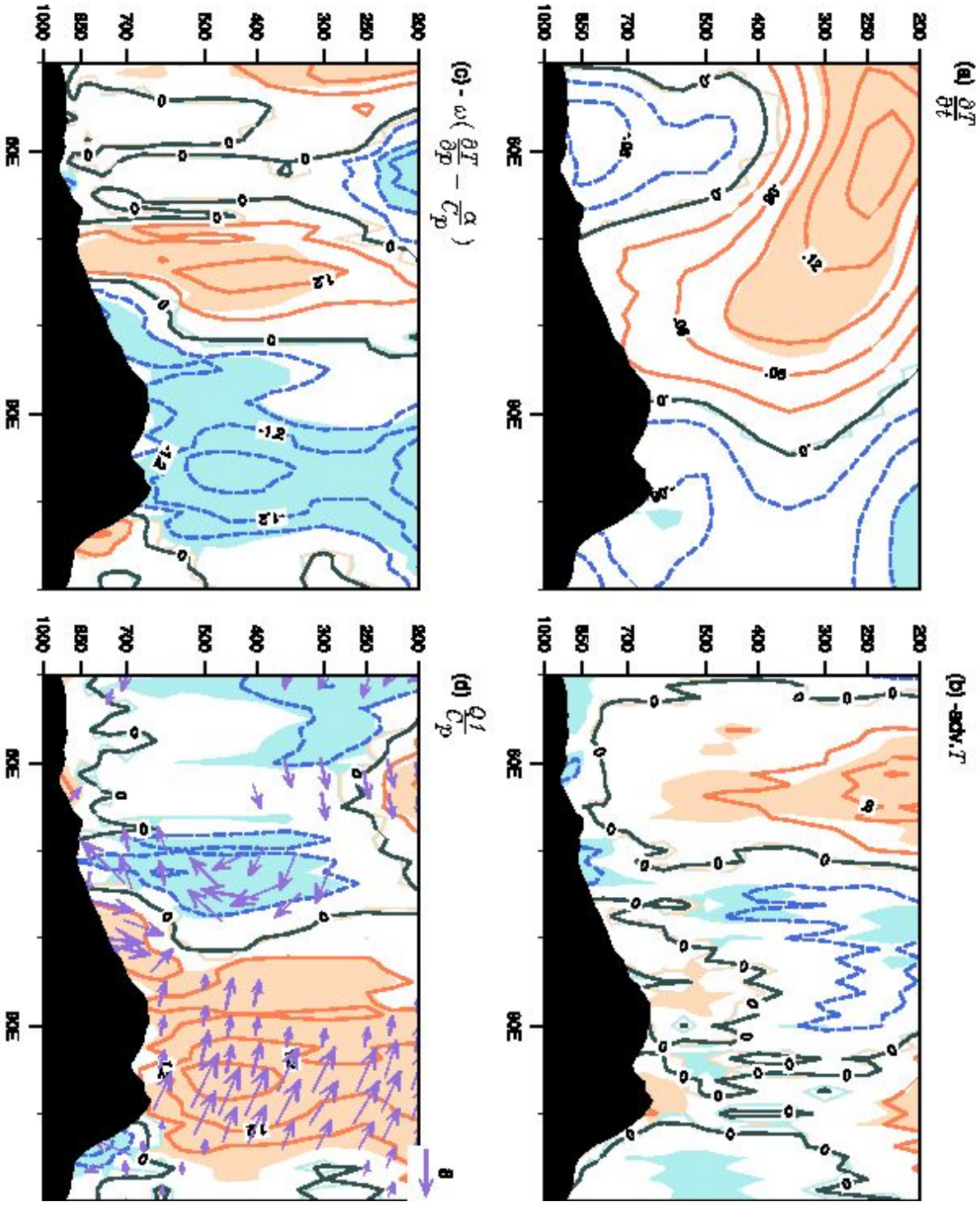

Figure 6

Composite differences in the meridionally averaged (25°–40°N) temperature budget between the positive and negative seesaw pattern of diabatic heating over the TP: (a) temperature tendency (∂T/∂t); (b) horizontal advection of temperature (-adv.T); (c) adiabatic heating (ω term); and (d) diabatic heating (Q_1/c_p (contours, units: K day−1) and zonal circulation (vectors, units: v in m s−1, -3ω in 10−2 Pa s−1). The orange, light blue shading and purple vectors indicate statistical significance at or above the 95% confidence level. The black shading indicates the topography

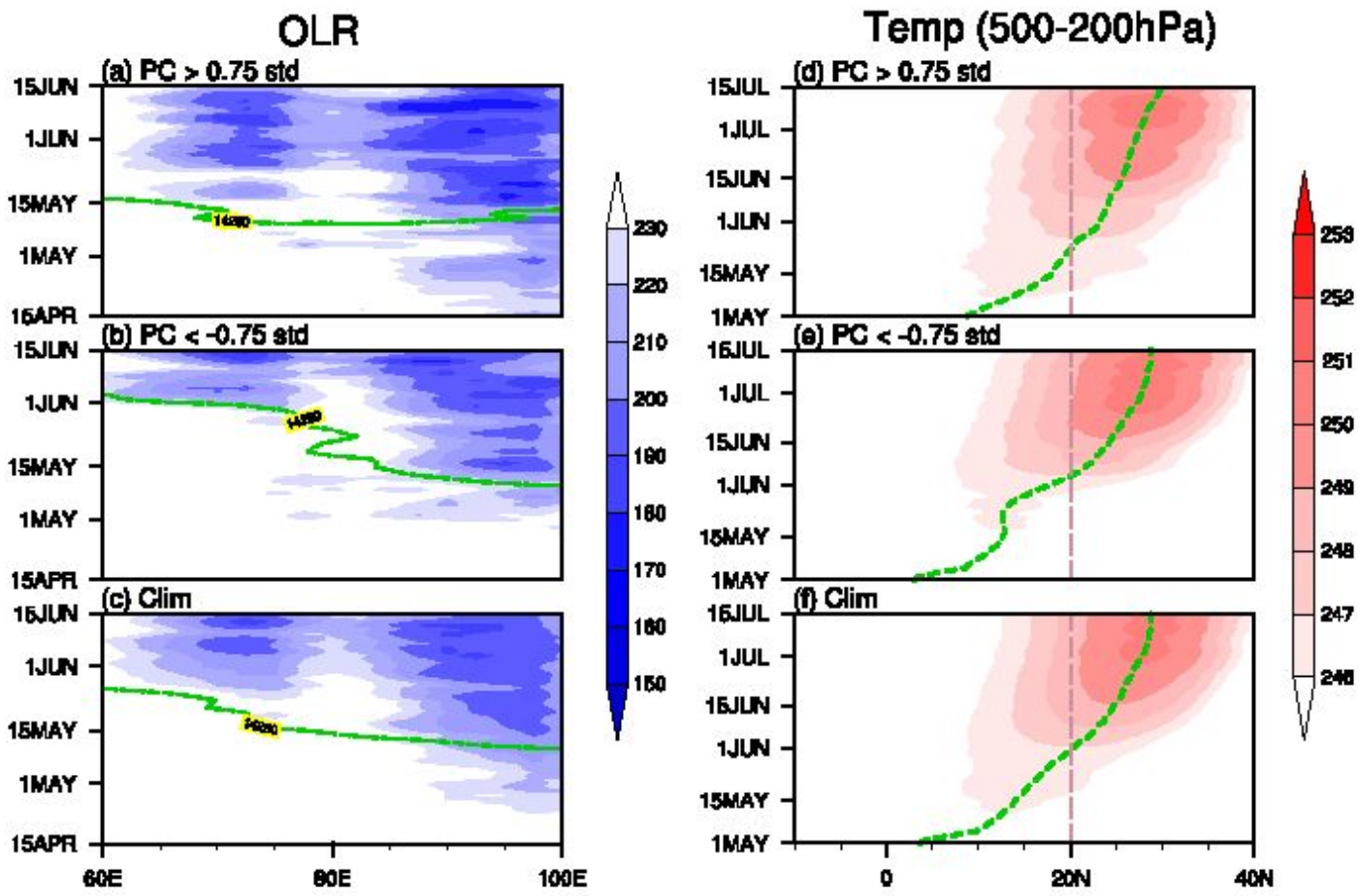

Figure 7

Composite evolution of (a–c) meridionally averaged (5°–15°N) OLR (shading, units: W m–2) and (d–f) zonally averaged (50°–90°E) temperature, vertically averaged over 500–200 hPa (shading, unit: K) for (a, d) PC > 0.75 standard deviation years, (b, e) PC < −0.75 standard deviation years and (c, d) the climatological mean. The green curves in (a–c) indicate the 14280 geopotential height at 20°N, and in (d–f) denote the maximum ridge line. The light pink denotes 20 °N

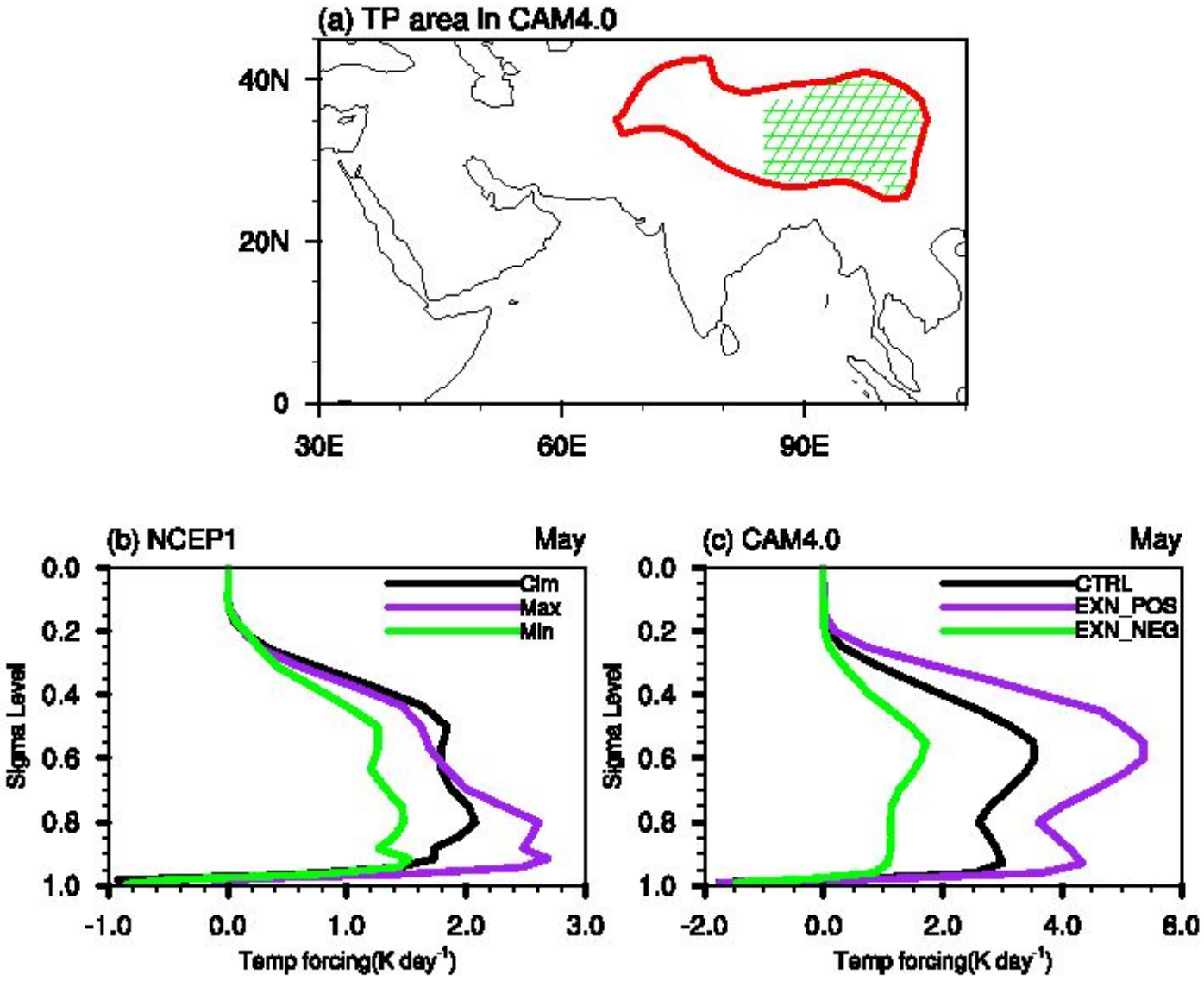

Figure 8

(a) The heating area (green meshed shading; 20°–40 °N, 85°–105 °E) over the Tibetan Plateau (> 1500 m) in the sensitivity runs. (b, c) Vertical profile of temperature tendency due to convection (units: K day−1) averaged over the areas in (a) based on (b) NCEP1 datasets (the black line represents the climatological mean value, the purple line represents the strongest value, and the green line represents the weakest value during 1979–2016) and (c) model simulation (the black line represents the CTRL value, the purple line represents the strong sensitivity experiment value (EXN_POS), and the green line represents the weak sensitivity experiment value (EXN_NEG). The black contours in (a) and (b) indicate the 2000 m topographic height

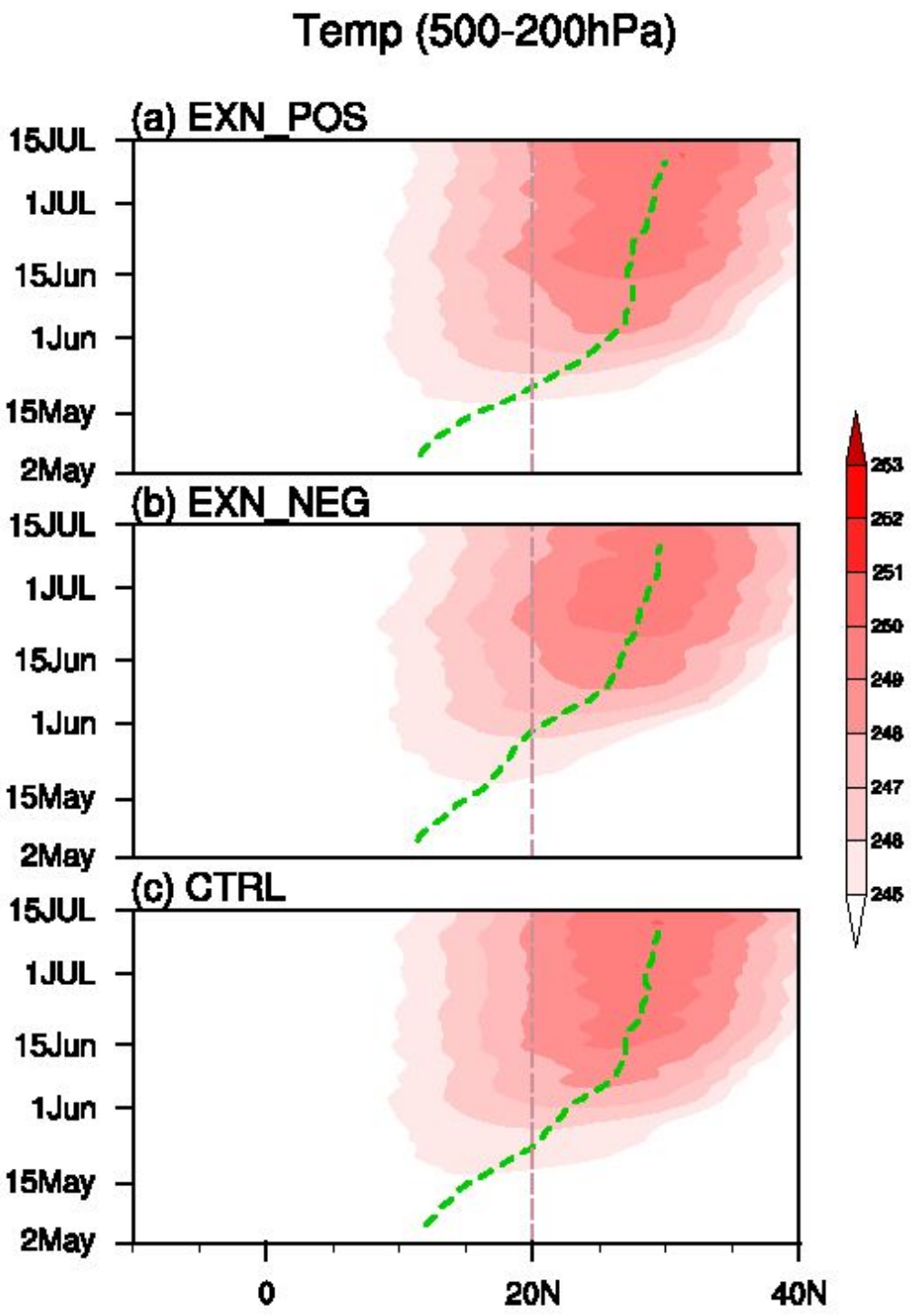

Figure 9

Zonally averaged (50°–90 °E) temperature, vertically averaged over 500–200 hPa (shading, unit: K) for (a) EXP_POS, (b) EXP_NEG and (c) CTRL. The green curves indicate the maximum ridge line. The light pink line denotes 20°N

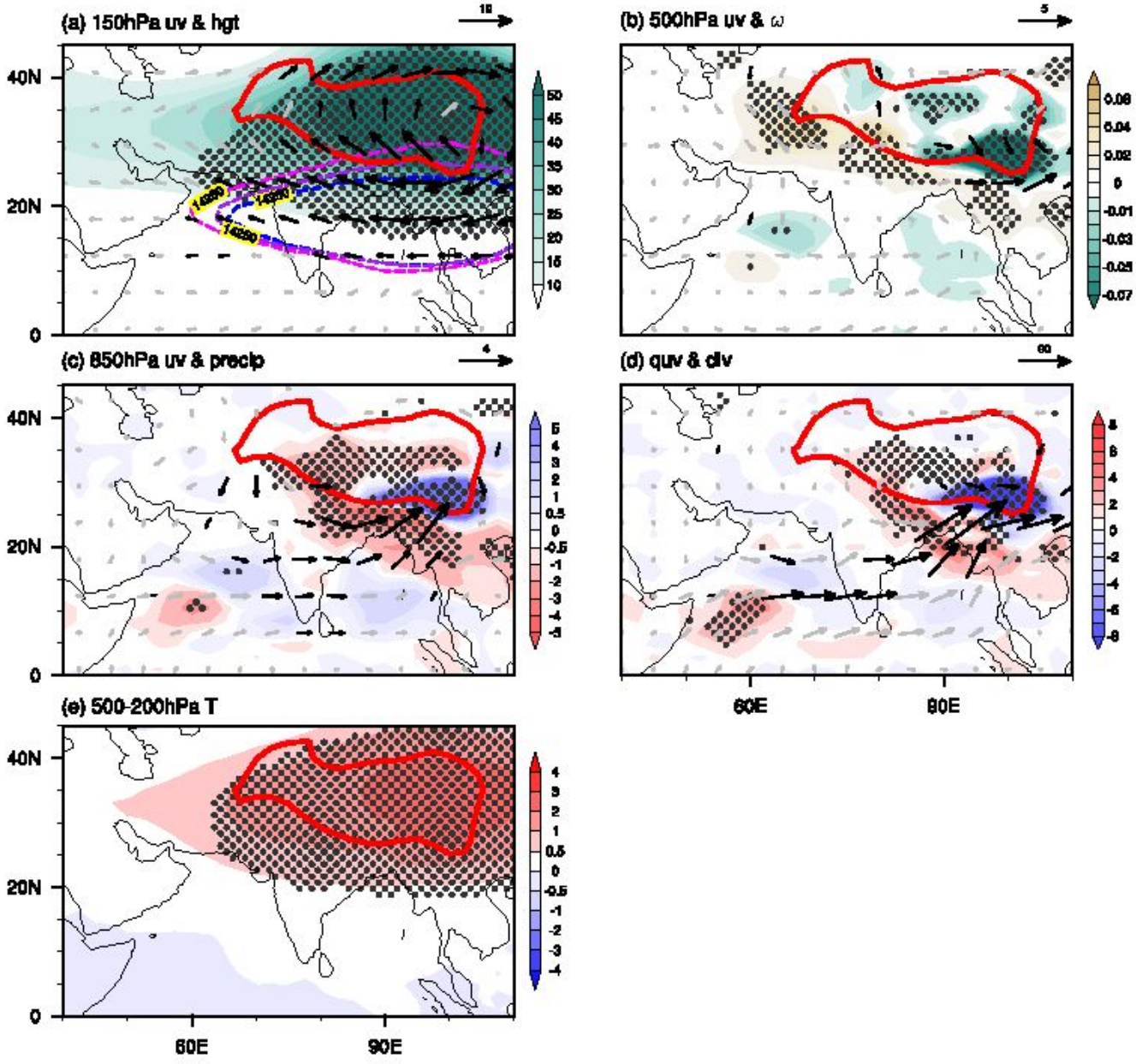

Figure 10

Differences in May quantities between EXP_POS and EXP_NEG: (a) 150-hPa geopotential height (shading, unit: gpm) and 150-hPa wind (vectors, units: m s−1); (b) 500-hPa vertical velocity (shading; units: Pa s−1) and 500-hPa wind (vectors, units: m s−1); (c) precipitation (shading, units: mm day−1) and 850-hPa wind (vectors; units: m s−1); (d) surface to 100-hPa vertically integrated moisture divergence (shading, units: 10−5 kg m−2 s−1) and moisture transport anomalies (vectors, units: kg m−1 s−1); (e) temperature, vertically averaged over 500–200 hPa (shading, unit: K). The purple, magenta and blue contours in (a) indicate the composite 14250 geopotential height in CTRL, EXP_POS and EXP_NEG, respectively. Black dotted areas and black vectors indicate statistical significance at or above the 90% confidence levels. The black contours in (a) and (b) indicate the 2000 m topographic height

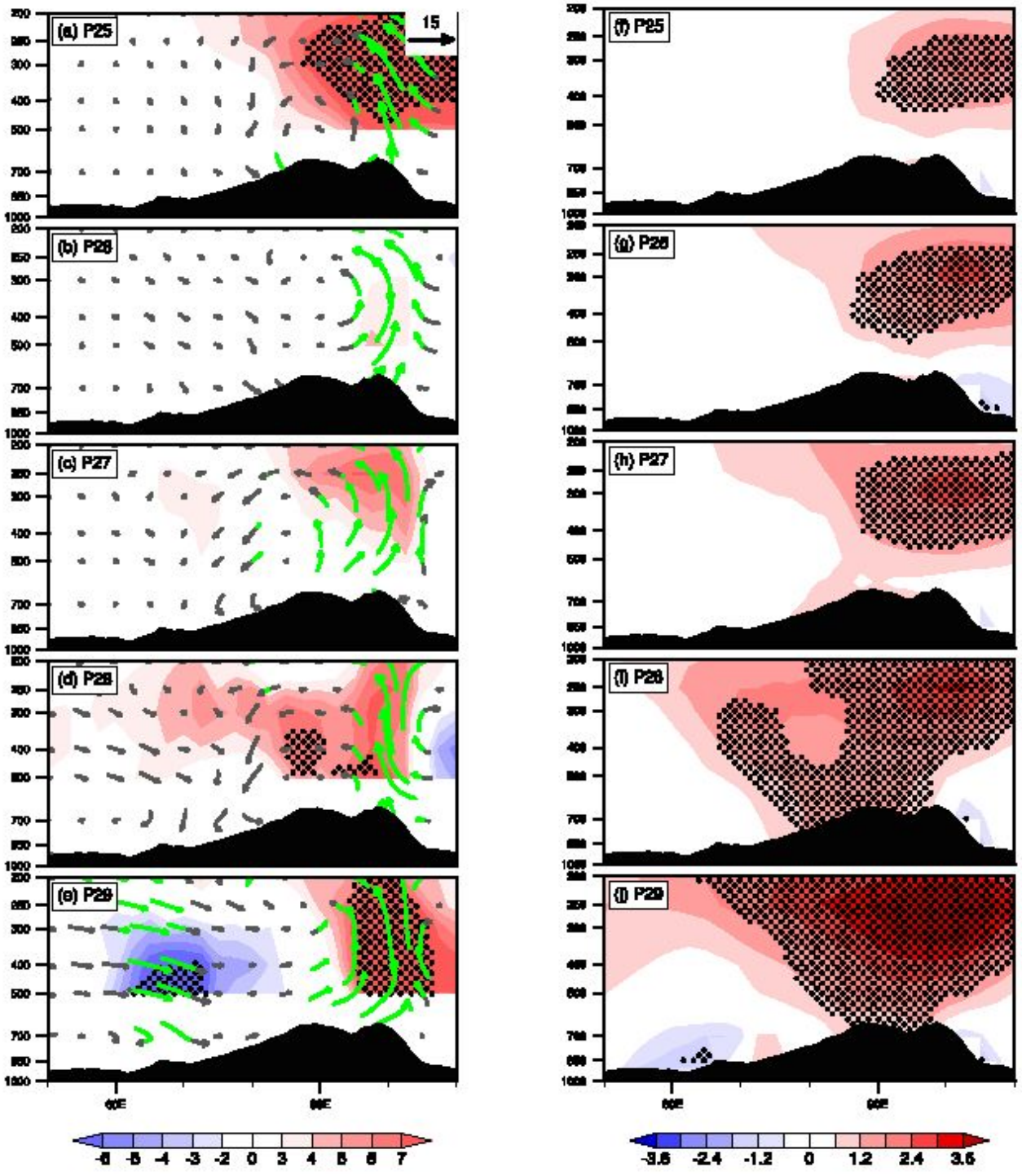

Figure 11

Differences in (a–e) meridionally averaged (25°–40°N) diabatic heating (contours, units: W m−2) and zonal circulation (vectors, units: v in m s−1, −3ω in 10−2 Pa s−1) and (f–i) air temperature (contours, unit: K) between EXP_POS and EXP_NEG from the 25th to 29th pentad. Black dotted areas and green vectors indicate statistical significance at or above the 90% confidence level

Supplementary Files

This is a list of supplementary files associated with this preprint. Click to download.

- 20210401supplementaryinformationhd.docx